Modification of turbulent transport by magnetic shear in cylindrical gyrokinetic simulations

E. Sánchez[1], X. Sáez[2], A. Soba[2], I. Calvo[1], R. Kleiber[3], R. Hatzky[4], F. Castejón[1], J. M. Cela[2]

[1] *Laboratorio Nacional de Fusión, Asociación EURATOM-CIEMAT, Madrid, Spain.*

[2] *Barcelona Supercomputing Center (BSC-CNS), Barcelona, Spain.*

[3] *Max-Planck Institut für Plasmaphysik, EURATOM-Association, Greifswald, Germany.*

[3] *Max-Planck Institut für Plasmaphysik, EURATOM-Association, Garching, Germany.*

The purpose of this work is to study the influence of the magnetic shear on the turbulent transport in cylinder geometry by means of several nonlinear simulations of ion temperature gradient (ITG) driven turbulence with the global three-dimensional gyro-kinetic code EUTERPE [1]. This code can simulate up to three kinetic species: ions, electrons and a third species with any charge and mass. The distribution function of each kinetic species is discretized using particles and a control variates scheme (δf) is used to reduce noise. In this work a plasma with only ions and electrons is simulated. The electrons are asumed to respond adiabatically and only electrostatic perturbations are taken into account. The evolution of the distribution function of ions is given by the Vlasov equation (no collisions are considered).

$$\frac{\partial f}{\partial t}+\frac{\mathrm{d}v_{\parallel}}{\mathrm{d}t}\frac{\partial f}{\partial v_{\parallel}}+\frac{\mathrm{d}\vec{R}}{\mathrm{d}t}\frac{\partial f}{\partial \vec{R}}=0, \tag{1}$$

where the evolution in time of $v_{\parallel}$ and $\vec{R}$ is given by the non linear equations

$$\frac{\mathrm{d}\vec{R}}{\mathrm{d}t} = v_{\parallel}\vec{b}+\frac{\mu B+v_{\parallel}^2}{B^*\Omega_i}\vec{b}\times\nabla B+\frac{v_{\parallel}^2}{B^*\Omega_i}(\nabla\times B)_{\perp}-\frac{\nabla\langle\phi\rangle}{B^*}\times\vec{b} \tag{2}$$

$$\frac{\mathrm{d}v_{\parallel}}{\mathrm{d}t} = -\mu\left[\vec{b}+\frac{v_{\parallel}}{B^*\Omega_i}(\nabla\times B)_{\perp}\right]\nabla B-\frac{q_i}{m_i}\left(\vec{b}+\frac{v_{\parallel}}{B^*\Omega_i}[\vec{b}\times\nabla B+(\nabla\times B)_{\perp}]\right)\nabla\langle\phi\rangle \tag{3}$$

$$\frac{\mathrm{d}\mu}{\mathrm{d}t} = 0, \tag{4}$$

μ being the magnetic moment per unit mass, which is a constant of motion; q_i and m_i are the ion charge and mass respectively, $\Omega_i = q_iB/m_i$ is the ion cyclotron frequency, $\vec{b}=\vec{B}/B$ is the unit vector in the magnetic field ($\vec{B}$) direction and $B^* = B+\frac{m_iv_{\parallel}}{q_i}\vec{b}\cdot\nabla\times\vec{b}$. $\langle\phi\rangle$ is the renormalized potential introduced in Ref. [2].

The system of equations is then closed with the quasineutrality equation:

$$\langle n_i\rangle - n_0 = \frac{en_0(\phi-\bar{\phi})}{T_e}-\frac{m_i}{q_i}\nabla\left(\frac{n_0}{B^2}\nabla_{\perp}\phi\right). \tag{5}$$

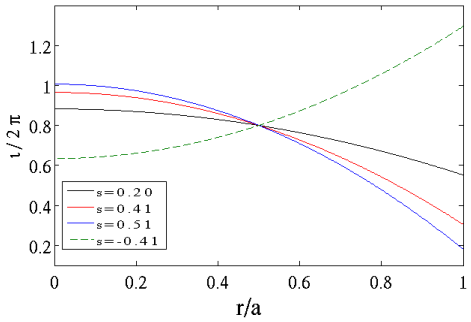

Figure 1: ι profiles used in this work labeled with $S = \hat{s}(r/a = 0.5)$.

Ideal ITG electrostatic simulations have been carried out in screw pinch geometry with flat density and electron temperature profiles while the ion temperature has a large gradient at half radius.

The physical parameters of all the simulations are: $B(0) = 2$ T, $L = 2\pi R$, $R = 4$ m, $a = 0.4$ m, $T_e(s = 0.25) = 3$ keV, where $s = \Psi/\Psi_0$ is the normalized toroidal flux used in the code as the radial coordinate.

Several screw pinch equilibria have been used, all of them having a rotational transform $\iota = 0.8$ at the position of maximum temperature gradient. Each equilibrium is calculated with a prescribed ι profile having a different value of the magnetic shear at this position. The magnetic shear is defined as $\hat{s} = \frac{r}{q}\frac{dq}{dr} = -\frac{r}{\tau}\frac{d\tau}{dr}$. The ι profiles used, labeled with $S = \hat{s}(r/a = 0.5)$, are shown in Fig. 1.

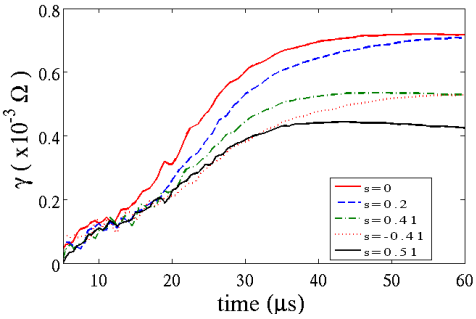

Figure 2: Growth rate of the electrostatic energy during the initial phase of the simulation.

All the simulations have been carried out using 540 million markers and a diagonal filter to reduce noise. The width of the filter in the poloidal direction (Δm) is adapted according to the local ι value to have the same cutoff in $k_{||}$ for all the ι (radii) values. The amount of markers used, together with the filter, allows to have a good signal quality, as measured by the signal to noise ratio, that is well above 10 during all the simulation. The signal to noise ratio is defined here as the ratio between the average spectral power of the modes in the filter divided by the average spectral power of the modes outside the filter (discarded at each time step in the simulation).

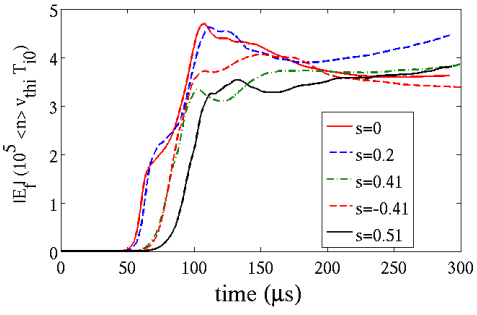

Figure 3: Electrostatic energy.

In the linear regime the magnetic shear shows a stabilizing effect, in agreement with theory [3]. The growth of the electrostatic energy is faster in the cases with lower magnetic shear ($S = 0.2, S = 0$) than for higher (absolute) values ($S = \pm 0.41, S = 0.51$) as shown in Fig. 2.

The sign of magnetic shear does not seem to affect the linear growth rate of ITG modes since the electrostatic energy shows similar growths for the $S = \pm 0.41$

cases.

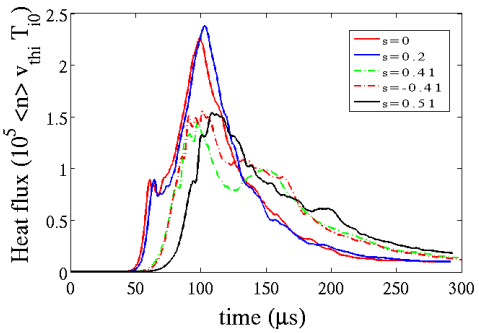

Figure 4: Average radial heat flux versus time.

The electrostatic energy is observed to nonlinearly saturate at lower values in simulations with larger shear values than in those with low shear (see Fig. 3).

An average radial heat flux is defined as $F = \langle v^2 v_r \rangle$, where $\langle\rangle$ means average for all the markers used in the simulation. This average heat flux is larger in the cases with larger magnetic shear (see Fig. 4) for late times in the nonlinear phase after the transition. This resembles the results observed in cylinder simulations [4, 5], where β showed a stabilizing effect in the linear growth rates but the heat flux increased with β. It also suggests a possible relation to the stiffnes observed in profiles [6, 7]. Profiles have been observed to be less stiff when the magnetic shear is small and also some recent results point out that a low magnetic shear facilitates the development of transport barriers [8]. We can speculate that as the flux is lower with low shear, the profiles will relax more slowly, thus giving a smaller slope in a power-gradient curve. However additional power driven simulations would be necessary to confirm this idea.

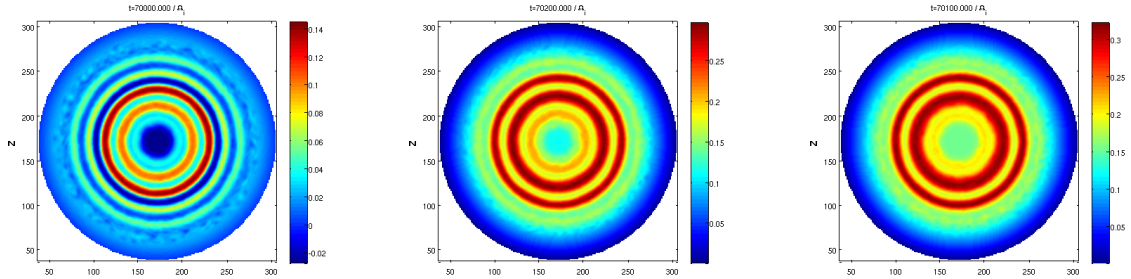

Figure 5: Electrostatic potential in the R-Z (poloidal) plane in the nonlinear phase of the simulation for the zero shear (left), $S = 0.4$ (middle) and $S = 0.5$ (right) cases.

In the nonlinear phase zonal perturbations in the potential appear. These zonal structures (Fig. 5) have a smaller radial scale for the low shear simulations (see Fig. 6). This results is not surprising if we take into account that the linear theory predicts a decrease in k_r with shear [3].

To look into more detail at these results we have calculated the fluctuations of the potential by subtracting the flux surface average to the total potential. An inverse cascade is observed in the spectrum of potential fluctuations in the nonlinear phase for all the cases, peaking at lower k values as the simulation evolves in time. In the higher-shear cases the potential fluctuations in the (n,m) plane (supressing the flux surface average) show smaller scales (higher k) as compared

to the low-shear cases. The amplitude of the fluctuations is also larger in the cases with higher shear.

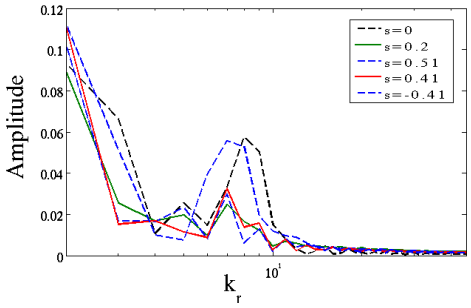

Figure 6: K_r spectra of the full electrostatic potential.

We find that the average heat flux is very similar in cases with different sign of the magnetic shear ($S = -0.41$ and $S = 0.41$) (see Fig. 4). However, in the case of negative shear ($S = -0.41$), the electrostatic potential exhibits a radial structure with a k_r larger than that of the $S = 0.41$ case and comparable to the case with $S = 0$ (Fig. 6). The spectra of fluctuations peaks at similar scales and the fluctuations have similar amplitude in both cases. The fact that the cases with different sign in the shear give similar averaged heat flux but different zonal perturbations in the potential questions the idea that the heat flux is controlled or regulated by these structures. Further simulations with negative magnetic shear will be conducted to clarify these results.

References

[1] G. Jost et al. 26th EPS Conf. on Contr. Fusion and Plasma Physics, Maastricht, 14 - 18 June 1999. ECA Vol.23J (1999) 1093.

[2] T. S. Hahm. Nonlinear gyrokinetic equations for tokamak microturbulence. Physics of Fluids 31, 2670, 1988.

[3] S. Hamaguchi, W. Horton. Phys Fluids B, 2, 1833 (1990).

[4] S. Sorge. Plasma Physics and Controlled Fusion 46, 535 (2004).

[5] E. Sánchez, R. Kleiber, R. Hatzky, A. Soba, et al. IEEE Transaction on Plasma Science 38, 2119 (2010).

[6] P. Mantica, D. Strintzi, T. Tala, C. Giroud et al. Phys. Rev. Lett. 102, 175002 (2009).

[7] F. Wagner, S. Baumel, J. Baldzuhn, N. Basse, R. Brakel et al. Physics of Plasmas 12 (2005).

[8] F. Militello, M. Romanelli, J. Connor & R. Hastie, R. Nuclear Fusion, 51, (2011).